JOURNAL OF CATALYSIS 100, 401–413 (1986)

Epoxidation of Ethylene over Ag–NaCl Catalysts

AKIMI AYAME,*,[1] TAKASHI YOSHIDA,*,[2] MASATSUGU YAMAGUCHI,*,[3] HIROYUKI MIURA,*,[4] YUKIO SAKAI,† AND NAOHIRO NOJIRI†

*Department of Industrial Chemistry, Muroran Institute of Technology, Muroran, Hokkaido 050; and †Mitsubishi Petrochemical Company Ltd., Central Research Laboratory, Ami-machi, Inashiki-gun, Ibaragi 300-03, Japan

Received December 29, 1983; revised April 1, 1986

Epoxidation of ethylene over sodium chloride-doped and granular sodium chloride-supported silver catalysts was performed at atmospheric pressure using conventional flow reactors. Although the stationary activity was somewhat low, each type of catalyst has shown high selectivity, 84–87%, under an ethylene-rich atmosphere. The selectivity was almost independent of reaction temperature, contact time, and catalyst composition. The total reaction rate rose exponentially with temperature until an apparent activation energy of 75.3 kJ mol^{-1} was obtained. Under oxygen-rich atmospheres, marked drops in activity were observed. In exposing the deactivated catalysts to a stream of hydrogen, carbon dioxide was desorbed. The strongly enhanced adsorption of carbon dioxide promoted the formation of silver chloride. Silver particles on the granular sodium chloride were homogeneously dispersed and ~200 nm in size. In addition, the crystallite size of silver was 43–50 nm, which was not altered after the reaction or even after heating at 673 K in oxygen gas. In a pulse reaction using an ethylene-rich gas mixture, acetaldehydes other than ethylene oxide were formed, and, as the catalyst surface had been oxidized by irreversible adsorption of oxygen, the formation of carbon dioxide was promoted and that of acetaldehyde decreased.

INTRODUCTION

About 20% of the reacted ethylene is lost as combustion products in the commercial production of ethylene oxide. From the viewpoint of more effective use of hydrocarbon resources, new catalysts with selectivity higher than that of the present catalysts should be prepared in the near future. With respect to the direct epoxidation of other light olefins, the problem is more important.

In the preceding works (*1*, *2*), the following facts were ascertained: catalysts prepared from silver(I) oxide and sodium chloride showed very high selectivity albeit at a somewhat low activity in a wide range of catalyst composition; the reduced (fresh) catalysts consisted of NaCl and metallic Ag; and each element in the surface layers was likely to form its oxidation state by the existence of oxygen contaminants. We are interested in further detailed characterizations of the catalyst surfaces. At the present time the most important goals are to determine the stationary states obtained in the epoxidation over catalysts and to reveal the various relationships among activity, selectivity, and several reaction conditions. In the present study, an attempt was made to characterize the time and temperature dependence of the catalytic activity and selectivity of Ag · NaCl and Ag/NaCl catalysts, the contact time effects, the origins of deactivation, the shape of silver particles, and some points of the reaction mechanism.

[1] To whom correspondence should be addressed.

[2] Present address: Nippon Core Co. Ltd., Sapporo, Hokkaido 061-24, Japan.

[3] Present address: Chisso Corporation, Minamata R&D., Minamata, Kumamoto 867, Japan.

[4] Present address: Daisel Chem. Ind. Co., General Research Laboratory, Himeji, Hyogo 671-12, Japan.

EXPERIMENTAL

Ag · NaCl Catalysts

Silver oxide (Ag_2O) was mixed well with an aqueous solution of NaCl, dried, and

0021-9517/86 $3.00

TABLE 1

Results on Epoxidation of C_2H_4 by the Flow Reactor System Using ORF-1

Catalyst[a]	Catalyst Comp.[b]	Reduction temp. (K)	Surface area ($m^2\ g^{-1}$)	Catalyst weight (g)	Reactor	Flow rate (ml min^{-1})	Reaction temp. (K)	Initial[c]		At 6 h[d]	
								X_{et}[e] (%)	$(EO)_{ro}$[f] (%)	X_{et} (%)	S[g] (%)
Cat-A3	0.04	608	0.28	0.20	I	4.2	523	—	—	4.9	86.6
				0.20	I	4.2	543	12.9	94.6	8.3	86.4
Cat-A1	0.04	723	0.29	0.23	I	4.1	543	11.4	96.0	5.5	81.3
Cat-A6	0.04	773	0.18	0.20	I	4.3	543	8.4	91.3	—	—
Cat-I	0.1	673	0.34	0.23	I	4.1	543	13.3	96.2	6.9	85.0
Ag-Sch-5	2.1	773	—	0.50	II	4.1	543	31.3	99.5	7.6	84.8
Ag-Sch-9	2.8	773	0.12	4.32	II	9.1	543	52.2	99.2	17.5	87.4
Ag-Sch-4	4.2	773	—	0.52	II	3.9	543	24.3	99.2	3.5	86.3
Ag-Sch-6a	8.3	773	—	0.53	II	4.1	543	13.8	97.3	3.9	85.0
Ag-Sch-6b	8.3	673	—	0.53	II	4.1	543	13.1	96.8	3.9	82.2
Ag-Sch-6c	8.3	843	—	0.53	II	4.0	543	12.9	98.5	3.3	84.4
Ag-Sch-6d	8.3	923	—	0.53	II	4.2	543	5.2	93.0	—	—

[a] Cat-series is Ag · NaCl catalyst (powder) and Ag-Sch-series is Ag/NaCl catalyst.
[b] Mole ratio of NaCl to Ag.
[c] Data at 15–20 min after the beginning of reaction.
[d] Data at 6 h after the beginning of reaction.
[e] Total ethylene conversion.
[f] Concentration ratio of C_2H_4O to (C_2H_4O + $\frac{1}{2}$ CO_2) at the outlet of the reactor.
[g] Selectivity to C_2H_4O ($S \doteq (EO)_{ro}$ at reaction times >4 h).

then powdered. The powder was preliminarily reduced by exposing it to a stream of H_2 at 333 K for 20 h. The temperature was subsequently elevated at a rate of 2.5 K min^{-1} and finally kept at a given temperature in the range 608 to 923 K for 3 h. The particle size of the reduced catalysts was in the range 100 to 200 mesh. The bulk catalyst composition is given in Tables 1 and 2. The catalyst charged into the reactors was further reduced by H_2 for 20 to 60 min at 673 K.

Ag/NaCl Catalysts

Distilled C_2H_5OH was added to Ag_2O powder to form a paste-like mixture. Then, a specified amount of granular NaCl (32–100 mesh) was added to the mixture. The C_2H_5OH was evaporated by agitating the mixture of Ag_2O, NaCl, and C_2H_5OH on a hot plate at 343 to 363 K. Finally the dried mixture was reduced in the manner similar to that used for the Ag · NaCl catalyst. The catalyst composition is also described in Tables 1 and 2.

Gases

The purities of the gases used were 99.8% for C_2H_4, O_2, and N_2; 99.0% for CO_2; and 99.998% for He. Ethylene oxide (EO) was prepared from $HOCH_2CH_2Cl$ (95%) and KOH (reagent grade) and purified twice by vacuum distillation. In the pulse reaction technique, He (99.9999%) purified by passage through an Oxisorb L column (Messer Grieheim Ind.) was used as a carrier gas.

Flow Reactors

The oxidation of C_2H_4 was performed at atmospheric pressure using two kinds of fixed bed flow reactors. One of the reactors (I) was made of Pyrex glass having an in-

TABLE 2

Results on Epoxidation of C_2H_4 Using ERF and Reactor I

Catalyst	Catalyst comp.	Reduction temp. (K)	Surface area ($m^2 g^{-1}$)	Catalyst weight (g)	Flow rate (ml min^{-1})	Reaction temp. (K)	Initial			Stationary state			
							X_{et} (%)	X_{ox}[a] (%)	S (%)	X_{et} (%)	X_{ox} (%)	S (%)	Time[b] (h)
Cat-A3	0.04	608	0.28	0.20	3.8	503	0.70	1.86	89.3	0.62	1.59	86.8	1
				0.20	3.8	543	2.48	7.54	86.1	2.30	6.85	85.8	0.5
Cat-A1	0.04	723	0.29	0.20	4.0	543	1.30	4.81	80.0	1.29	4.82	79.8	1
Cat-J	0.2	773	—	0.20	4.2	543	2.35	6.69	88.9	2.06	6.13	86.9	0.5
Cat-Q	0.5	773	—	0.20	3.7	543	2.56	7.70	89.9	2.34	7.15	87.4	1
Cat-R	2.8	773	—	0.20	4.3	543	1.46	5.18	91.1	1.03	3.68	88.3	1
Ag-Sch-5	2.1	773	—	0.21	3.9	543	2.22	5.14	88.4	2.19	6.59	86.7	0.5
Ag-Sch-9	2.8	773	0.12	0.20	3.6	503	0.24	0.67	86.9	0.24	0.68	86.5	0.5
				0.20	3.8	543	1.23	3.28	87.4	1.02	2.93	86.2	0.7
				0.40	2.1	543	2.21	6.98	86.6	2.08	6.65	86.1	0.7

[a] Total oxygen conversion.
[b] Time required to reach a stationary state. Other symbols and notes are given in Table 1.

side diameter of 4 mm. A glass thermocouple shield (4 mm o.d.) was attached to the reactor. About 0.2 g of the Ag · NaCl and Ag/NaCl catalysts was charged into the reactor. The height of the catalyst bed was 8–18 mm. For Ag/NaCl catalysts another reactor (II, 10 mm i.d.) having a glass thermocouple shield at its center was also used. In this case, 0.5–4.3 g of the catalyst (~6 mm in height) was packed into the reactor.

The reaction temperature was represented by the mean value through the catalyst bed, which was controlled within 2 degrees. The differences between maximum and minimum temperatures through the bed were smaller than 2% of the reaction temperature. Consequently, heat transfer effects were considered to be negligible.

Three kinds of reactant mixtures were used: oxygen-rich feed 1 (ORF-1) of 2.8 vol% C_2H_4 and 17 vol% O_2 balanced by N_2; oxygen-rich feed 2 (ORF-2) of 2.8 vol% C_2H_4 and 80 vol% O_2 balanced by N_2; and an ethylene-rich feed (ERF) of 43 vol% C_2H_4 and 12 vol% O_2 balanced by He. No organic chlorides were added to the feeds.

Analysis of gases were performed by a gas chromatograph equipped with DOP and Porapack Q column in series at 373 K.

Pulse Reactor

The reactor was a Pyrex glass U-tube, 3 mm i.d., in which 0.1 g of the Ag · NaCl catalyst was packed. The flow rate of the helium carrier was 15 ml min^{-1}. A reactant mixture of the same composition as that of ERF was prepared using purified gases. Pulse size was 50 μl and pulse interval, 30 min. The product gases trapped at 77 K for 10 min were analyzed by a gas chromatograph equipped with Porapack QS, since the effusion of carbon dioxide from the catalyst bed was slow due to its strong adsorption behaviors.

SEM and XRD

Secondary electron micrographs of the Ag/NaCl catalysts were measured with a Hitachi S-550. XRD patterns of the Ag · NaCl catalysts were measured with a Rigaku-Denki D-6C (Cu$K\alpha$). The crystallite size of metallic Ag was determined from the XRD peak of Ag(111) using Scherrer's equation.

RESULTS AND DISCUSSION

Oxygen-Rich Feeds

Typical curves of the time dependence of

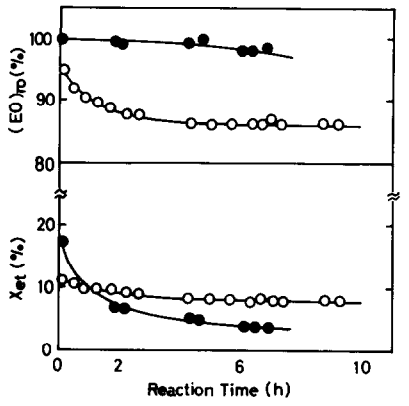

FIG. 1. Time dependences of catalytic activity and $(EO)_{ro}$. (○) Cat-A3 (0.20 g), 543 K, 4.2 ml min^{-1}, ORF-1, Reactor I. (●) Ag-Sch-9 (4.32 g), 503 K, 9.1 ml min^{-1}, ORF-2, Reactor II.

activity and $(EO)_{ro}$ obtained over Cat-A3 are shown in Fig. 1, where $(EO)_{ro}$ is the concentration of EO in the gaseous part of product. At about 6 h after the starting of the reaction, the catalyst manifested a comparatively stable activity state and $(EO)_{ro}$ was nearly equal to the selectivity to EO. However, a gradual drop in activity was observed for a long time. At longer contact times, the decay in activity was more remarkable. When ORF-2 was employed, the decay was very vigorous, although $(EO)_{ro}$ was very large. All of Ag · NaCl and Ag/NaCl catalysts have shown behavior similar to that mentioned above.

Table 1 indicates the activity and selectivity or $(EO)_{ro}$ which were obtained at 5 to 8 h, in comparison with their initial values. The high value of $(EO)_{ro}$ at the earlier stage was attributed to the discrepancy in carbon balance, which had arisen from the enhanced adsorption of CO_2 or its precursors on the catalysts. Figure 2 indicates the discrepancy over Ag-Sch-7 (the mole ratio of NaCl to Ag is 16.6) and the effusion curve of CO_2 in exposing the used catalysts to a stream of H_2. The integrated area of the shaded part corresponded to 2.34×10^{-5} mol of C_2H_4. The integral amount of CO_2 desorbed for 50 min was 3.82×10^{-5} mol; 3.8×10^{-6} mol as C_2H_4 and C_2H_4O was also effused, simultaneously. In this case the integral total conversion and the net selectivity are 13.9 and 81%, respectively. Further, the used catalyst which had been exposed to a stream of H_2 indicated the original activity and $(EO)_{ro}$.

Ethylene-Rich Feed

All of the catalysts showed small changes in activity and selectivity with reaction time, and within 1 h their stationary values were obtained (Table 2). Few significant differences in carbon balance were observed. The stationary selectivity, 84–87%, agrees with the maximum value, 85.7%, anticipated from the well-known mechanistic studies by Kilty and Sachtler (*3*). The relationship between stationary reaction rate expressed in a unit gram of Ag and catalyst composition was quite similar to that obtained over the fresh catalysts by the use of the pulse reaction technique (*2*). Also, the two different types of catalyst with the same composition had identical activity and selectivity (Cat-R and Ag-Sch-9).

Mass Transfer Effects

Plots of stationary total conversion against contact time using ERF are shown in Fig. 3. The stationary selectivity was almost independent of contact time, although the total conversion increased. At contact times smaller than 3000 g-cat · min mol-$C_2H_4^{-1}$, the plots were very close to a

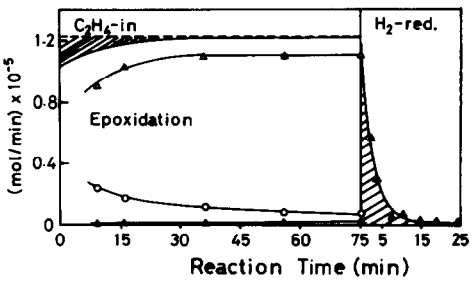

FIG. 2. Time dependences of moles of gaseous products and unreacted C_2H_4 observed over Ag-Sch-7 (2.36 g, 543 K, 9.64 ml min^{-1}, Reactor II), and the curve for effusion of CO_2 in exposing the used catalyst to a stream of H_2 (10 ml min^{-1}) at the same temperature. (○) C_2H_4O, (▲) CO_2, (△) unreacted C_2H_4.

TABLE 3

Variations of Activity and Selectivity with Various Treatments (Ag-Sch-9 Catalyst, 4.32 g)[a]

Activity before treatment		Treatment at 543 K			Activity just after treatment[b]		Activity 6 h after treatment		
		Gas	Flow rate (ml min^{-1})	Time (h)					
X_{et} (%)	S (%)				X_{et} (%)	S (%)	X_{et} (%)	S (%)	Time[c] (h)
17.5	86.6	0.3% C_2H_4O + 99.7% Air	8.9	1	10.7	79.3	18.1	85.8	6
18.1	85.8	2.0% C_2H_4O + 98.0% Air	11.2	4	11.0	84.5	17.8	86.5	6
15.8	87.6	Pure CO_2	10	0.5	19.6	75.4	16.1	86.8	1.5
16.1	86.8	Pure CO_2	10	1	20.5	84.3	15.5	86.6	11
18.4	85.6	Pure O_2	10	1	11.9	90.0	19.9	85.7	5
19.9	85.7	Pure O_2	10	1	11.7	88.2	21.8	85.8	6

[a] The epoxidation of C_2H_4 was carried out at 543 K and 10.4 ml min^{-1} using ORF-1 and Reactor II.
[b] Values at 15–20 min after the treatment.
[c] Time required to reach the newly stable activity state.

straight line. The open symbols in Fig. 3 for Cat-Al and Ag-Sch-9 denote the data measured using different amounts of catalyst. From the results, it was evident that concentration gradients had disappeared completely, except for those data which in the Arrhenius plots indicated zero activation energy at higher temperatures (Fig. 7). The total reaction rate estimated from the line for Cat-A3 is 9.3×10^{-6} mol-C_2H_4 g-cat^{-1} min^{-1}. The space–time yield of EO is 0.02 kg-EO kg-cat^{-1} h^{-1}, which is comparable to that obtained over Ag–Ba–Na, Cs, Rb, or K catalysts in the presence of $C_2H_4Cl_2$ (*4*).

Annealing Effect

Drops in activity with treatment at high temperatures were evaluated from several data for Cat-A and Ag-Sch-6 series (Table 1). The activity drop of the latter took place at very high temperatures compared to that of the former. The activity of Cat-A treated at higher temperatures declined significantly with reaction time.

Treatment with EO, CO_2, and O_2

It has been well known that silver catalysts are poisoned by the deposition of polymer-like hydrocarbons originated from adsorbed EO molecules and the poisoning takes place in the course of epoxidation (*5–11*). In the present work, a gas mixture of EO and O_2 was passed through the catalyst bed of Ag-Sch-9 at 543 K, which had

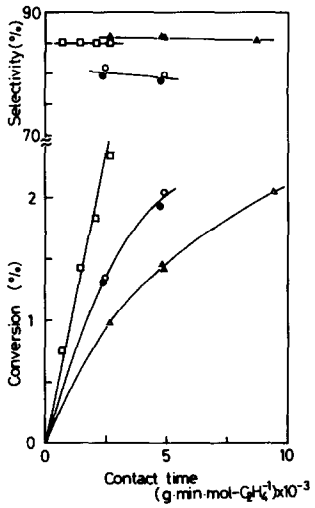

FIG. 3. Dependence of total conversion and selectivity on contact time at 543 K using ERF. (Circles) Cat-A1, (triangles) Ag-Sch-9, (squares) Cat-A3.

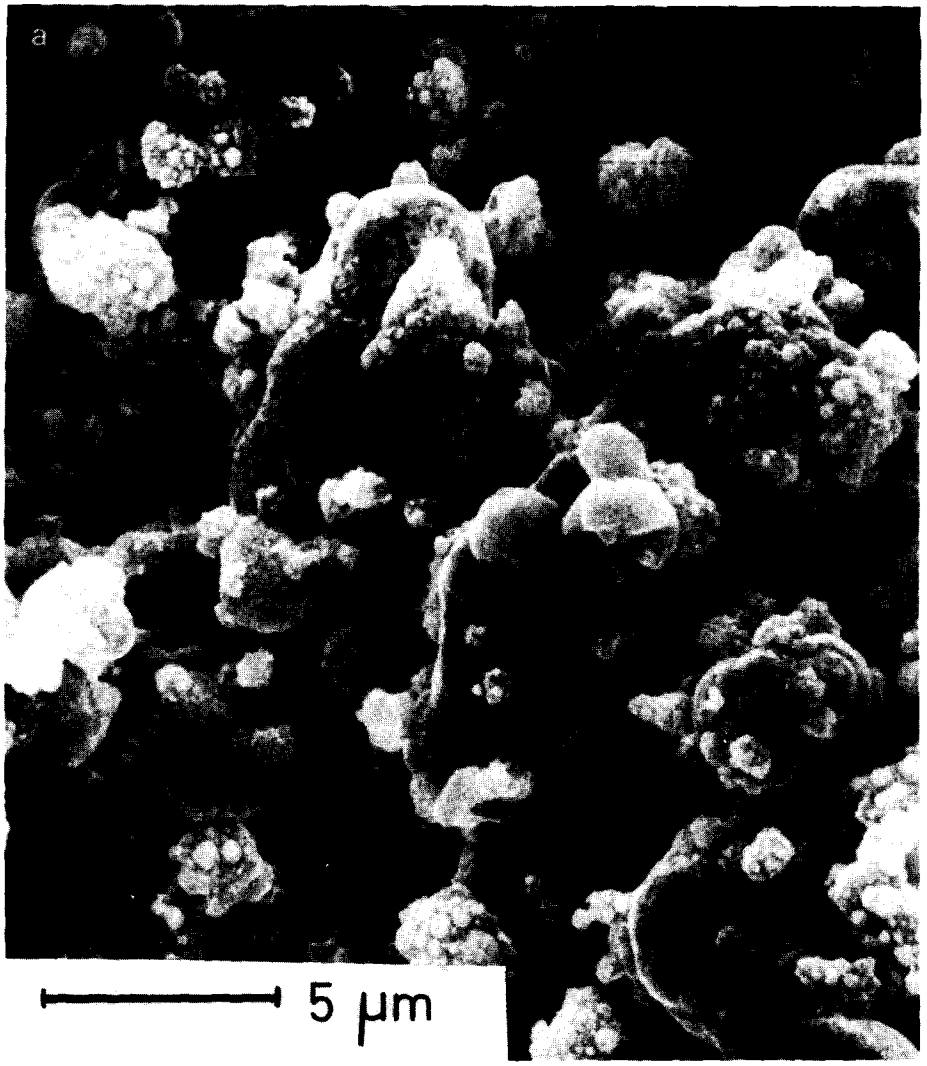

FIG. 4. Scanning electron micrographs of fresh Ag-Sch-9 catalyst.

previously been stabilized using ORF-1 at the same temperature. The conversion of EO to CO_2 was smaller than 2 mol%. After again switching the gas mixture to ORF-1, a large decay in activity was observed. During a continuance of the epoxidation the activity and selectivity were completely restored. These results suggest that no permanent deposition of polymer-like materials has taken place on the catalyst surface and that the adsorbed EO, that is, a combustion intermediate, decomposes slowly to CO_2 and H_2O during the reaction. The intermediate is considered to be a species identical to C_2H_4 adsorbed on oxygen adatom (*11, 21*).

Exposure of the Ag/NaCl catalyst to oxygen resulted in a marked decay in activity. The decay seems to be attributable to the low reactivity of oxygen which binds tightly with silver, sodium, or both atoms and/or dissolves in the surface layers. Similar behavior had been observed for Ag–K_2SO_4 catalysts (*12*).

The temporary elevation in activity of the catalyst treated with pure CO_2 was an unex-

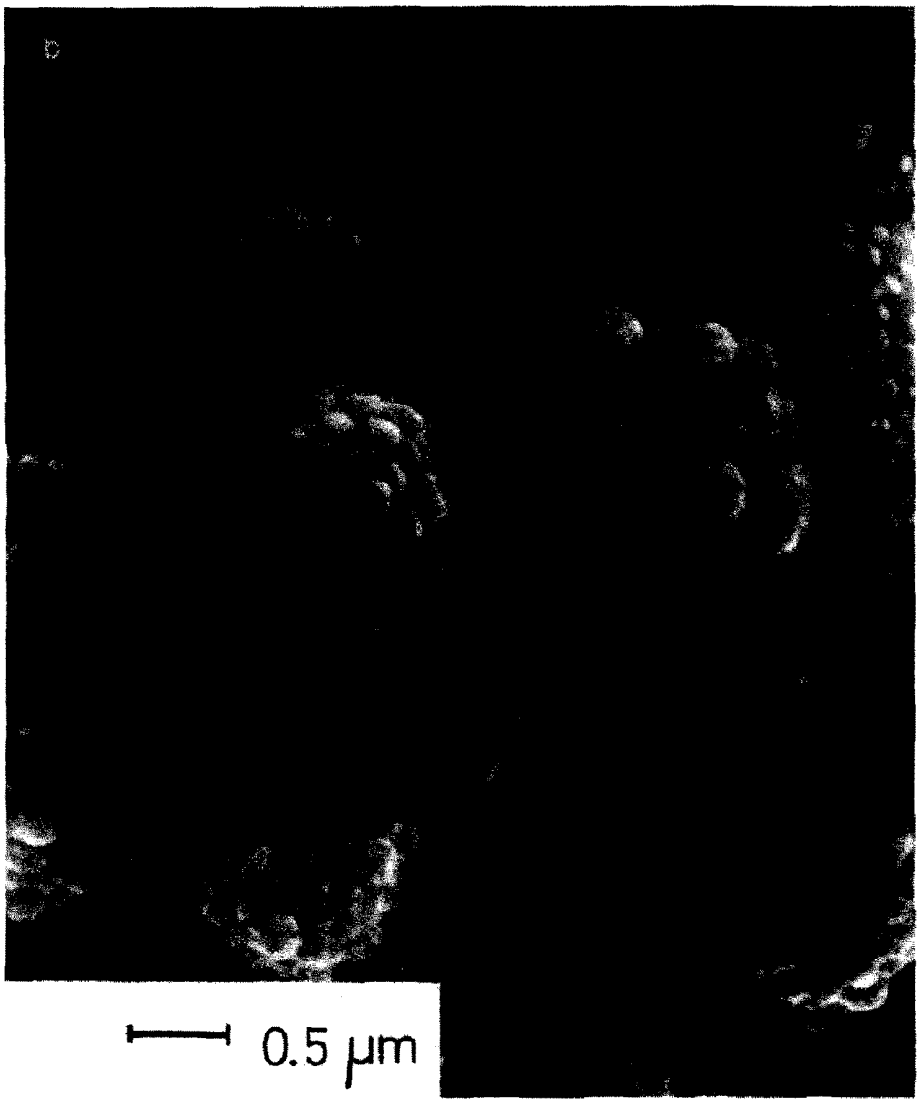

FIG. 4—*Continued.*

pected result. Perhaps, the surface atoms are partially reduced by the adsorption of CO_2, which may form sodium carbonate because of the absence of O_2 in the gas phase.

SEM and XRD

Scanning electron micrographs of fresh Ag-Sch-9 are shown in Figs. 4a and b. The small spherical particles (white or bright) are Ag, the diameter of which ranges from 50 to 200 nm (average 200 nm). Large smooth-surface particles of different shapes (dark) are NaCl crystals, which are 2–5 μm in size. Also, it can be seen that the Ag particles are firmly adhered and dispersed homogeneously on the NaCl surfaces. The degree of dispersion of Ag was estimated to be ~1%. It must be realized that supported Ag catalysts with high selectivity contain secondary Ag particles, 50–200 nm in size, which are dispersed homogeneously (*13*). Surprisingly, the particle size of Ag on the Ag/NaCl catalyst coincides completely with the characteristic size. Micrographs of the Ag-Sch-9 employed in the epoxidation

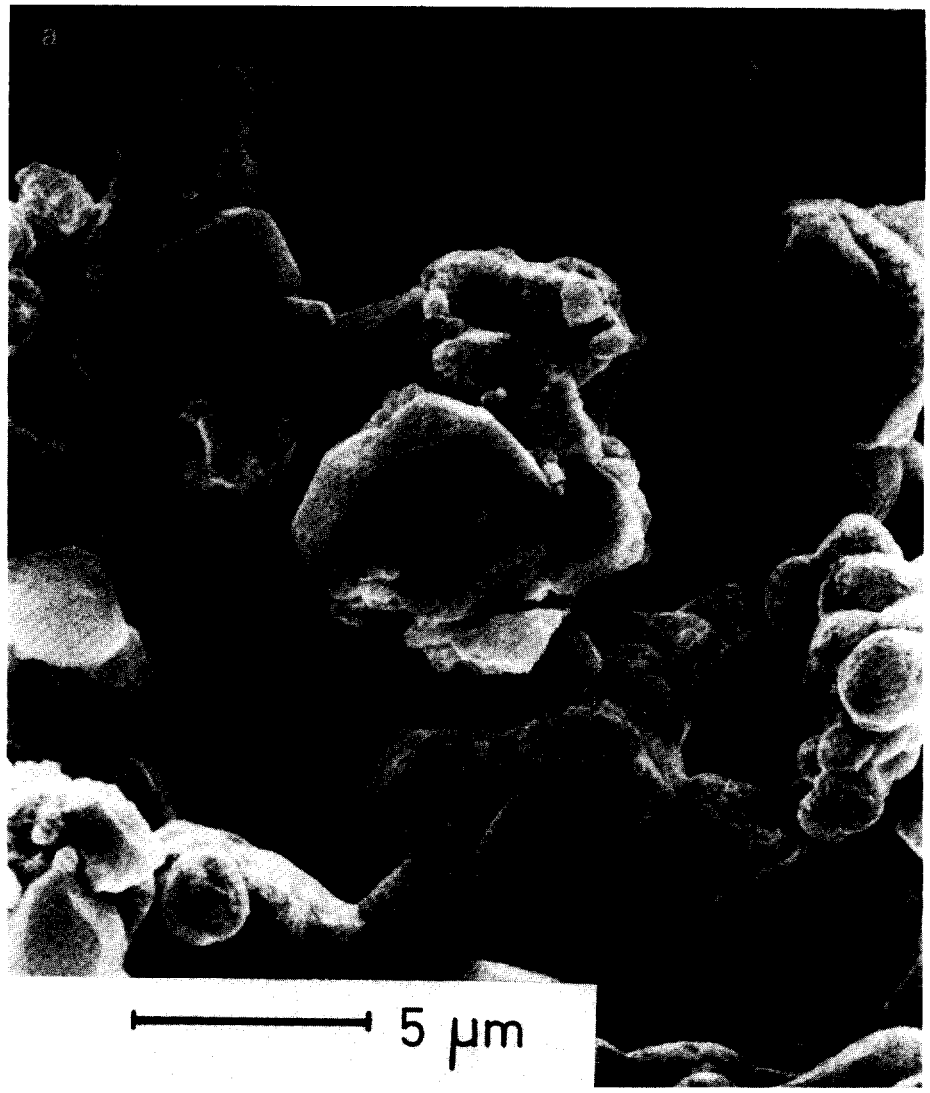

FIG. 5. Scanning electron micrographs of Ag-Sch-9 catalyst after epoxidation at 543 K for 2 days.

at 543 K for 2 days are shown in Figs. 5a and b. By comparing these micrographs with Figs. 4a and b, it can be found that the shape and size of Ag particles remain unaltered. A similar conclusion can be reached for NaCl particles.

In XRD measurements of fresh catalysts, peaks other than metallic Ag and NaCl have not been observed (*1*, *2*). Similar results were also obtained for the catalysts after reaction at 543 K for 4 h. However, in the case of several catalysts used in the reaction at 543 K for 2 or more days, XRD peaks of AgCl (2θ = 27.8, 46.2, and 54.8°) were clearly found. Diffraction peaks of Na_2CO_3 were not detected because of their weak intensities. Exposure of these used catalysts to a stream of H_2 caused the desorption of CO_2, the disappearance of AgCl XRD peaks, and then a restoration of activity.

The Ag crystallite size of Ag · NaCl catalysts, which was estimated from the Ag(111) peak (2θ = 38.1°), increased with

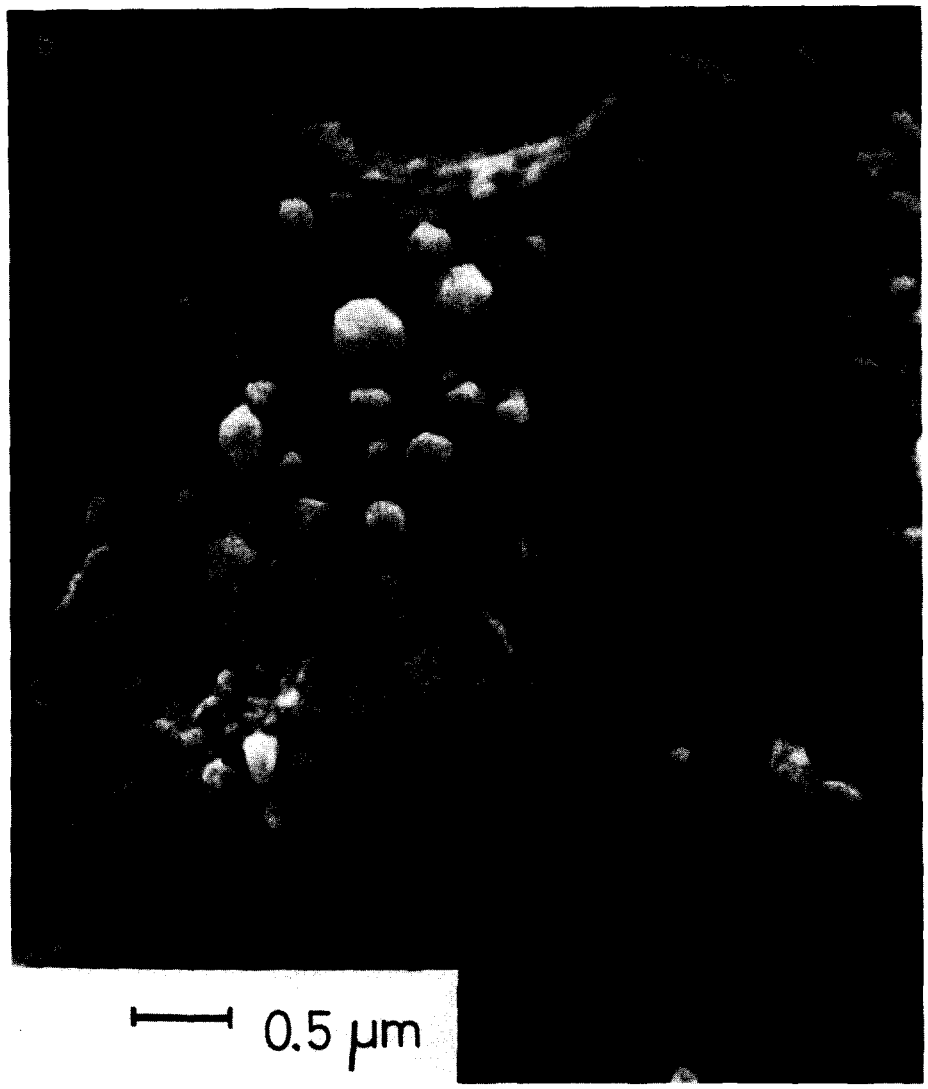

FIG. 5—*Continued.*

NaCl content and showed a constant value of 48 nm above NaCl/Ag = 1 (mole ratio) (Fig. 6). Specific activity changed with NaCl content in a manner similar to that described above, while selectivity reached a maximum of about 86% at NaCl/Ag = 0.04. The two types of catalyst with the same composition showed an identical Ag crystallite size of 47.5 nm (Cat-R and Ag-Sch-9).

The Ag crystallite size of Ag · NaCl catalyst remained unchanged after the reaction and even after exposure to O_2 at 523 K (Table 4). Pure Ag powder, however, increased in size after treatment with O_2, as revealed by Feller-Kniepmeier *et al.* (*14*), Seiyama *et al.* (*15*), and Presland *et al.* (*16*). The larger Ag crystallite size in Ag · NaCl catalysts than in pure Ag powder heated in O_2 implies that NaCl has inhibited the complete reduction of silver oxides in the course of catalyst preparation. In AES and XPS measurements reported earlier (*2*, *17*), XPS spectra of O 1*s* (531.3 to 532.0 eV

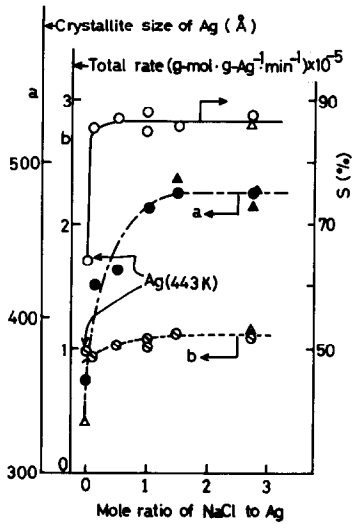

FIG. 6. Relationship between the crystallite size of Ag (----), activity (---), or selectivity (—) and catalyst composition. Activity and selectivity were measured at 543 K and 4 ml min^{-1} using ERF and a catalyst weight of 0.2 g. Ag(443 K) indicates data measured at 443 K over pure Ag powder catalyst. (Circles) catalysts reduced at 673 K for 3 h, (triangles) catalysts reduced at 773 K for 3h.

peak assigned to subsurface oxygen atom was predominant) and the AES peak of O for Ag · NaCl catalysts were not eliminated even after several overnight hydrogen reductions and outgassings at 673 K, while for pure Ag powder the O 1*s* spectra were negligible. Consequently, oxygen atoms persisting by strong ionic interactions with Ag, Na, and Cl are considered to promote the aggregation of Ag particles. As can be seen from Fig. 6 and Table 4, the catalysts with higher selectivity possess Ag crystallites of 42–50 nm. This fact agrees with the experimental results obtained for pure Ag by Wu and Harriott (*18*) and for alumina-supported Ag by Kanoh *et al.* (*19*).

Mechanisms

Total reaction rates and selectivities were plotted as a function of reciprocal temperature (Fig. 7). In the case of ORF-1, at temperatures lower than 543 K an apparent activation energy, 75.4 kJ mol^{-1}, was obtained for both EO and CO_2 formations since selectivity was almost constant. However, zero activation energy obtained at high temperatures shows that the process of diffusion of C_2H_4 to the catalyst surface is rate controlling, which causes a prominent decrease in selectivity. The activation energy estimated from the initial formation rates of EO (CO_2 detected was very small) was 44.8 kJ mol^{-1}, which agreed with that obtained in the previous work using the pulse technique (*2*). The discrepancy in activation energy reflects the differences in physicochemical properties between the

TABLE 4

Silver Crystallite Sizes of Ag · NaCl Catalyst and Pure Ag Powder Treated in a Stream of Several Gases

Catalyst	Crystal face (*hkl*)	Silver crystallite size (nm)				
		Before use[a]	After epoxidation[b]	After the subsequent reduction[c]	After treatment with oxygen[d]	After the subsequent reduction[c]
Ag · NaCl[e]	(111)	49	48	48	48	49
	(200)	43	43	—	43	43
Pure Ag	(111)	33	—	—	45	42
	(200)	29	—	—	38	40

[a] Catalysts were treated at 773 K in a stream of H_2 for at least 3 h.
[b] At 523 K for 4 h in a stream of ORF-1.
[c] At 673 K for 1 h in a stream of H_2.
[d] At 523 K for 4 h in a stream of pure O_2.
[e] Mole ratio of NaCl to Ag is 1.5 (Cat-N).

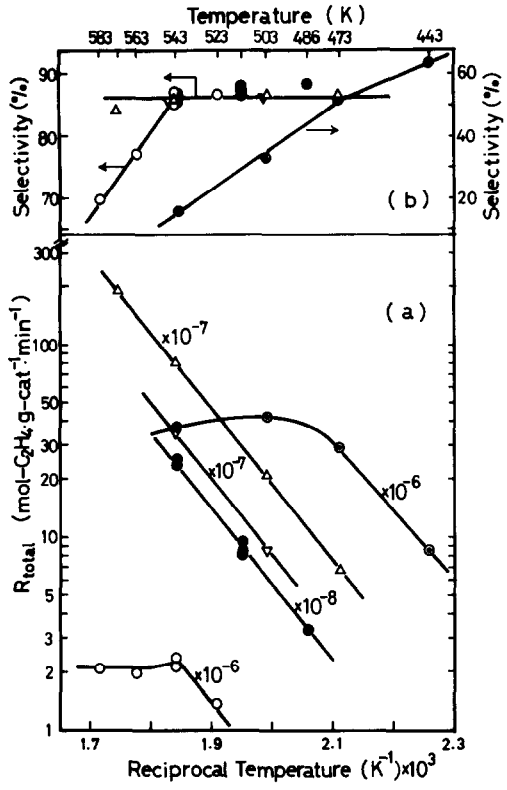

FIG. 7. Relationship between total reaction rate and reciprocal reaction temperature (a), and dependence of selectivity on reaction temperature (b), which were measured at contact times smaller than 2500 g-cat · min mol-$C_2H_4^{-1}$. (○) Cat-A3, ORF-1; (●) Ag-Sch-6a, ORF-1; (△) Cat-A3, ERF; (▽) Ag-Sch-9, ERF; (⊙) Pure Ag, ERF.

fresh catalyst surface and that after 6 h reaction. An increase in Ag particle or crystallite size anticipated as one of the origins of catalyst deactivation has not been observed. A good carbon balance was obtained on the catalysts after 6 h reaction, whereas on the fresh catalysts carbon dioxide or its precursors accumulated. In addition, the formation of AgCl has been ascertained on catalysts employed in lengthy epoxidations. From these results, it can be considered that the adsorption of carbon dioxide forms Na_2CO_3 causing the formation of AgCl-like species. Thus the following equilibrium would have been established:

$$2Ag + O_{ads} + CO_2\,(g) \rightleftharpoons Na_2CO_3 + 2AgCl. \quad (1)$$

The oxygen adatom would be bound to either Ag or Ag and Na (bridge type). No formation of AgCl takes place unless Ag has been oxidized sufficiently (*2, 17*). Since AgCl and Na_2CO_3 are inactive in the epoxidation, their formation would retard the reaction rate and result in an increase in the activation energy. The drastic drops in activity observed when ORF-2 was used (Fig. 1) are ascribed to the marked shift in the equilibrium to the right. In the case of ERF, Arrhenius plots with the same slope as mentioned above were also obtained. No mass transfer limitation was observed for Ag · NaCl and Ag/NaCl catalysts. Continuous exposure to ERF, seems to keep the catalyst surface in the equilibrium state, shifted moderately to the left in Eq. (1) because of the Na_2CO_3 decomposed by hydrogen treatment (Fig. 2). Consequently, the reaction time required to reach the stationary activity states is shorter than that in the case of ORF-1 (Table 2). Under similar conditions, the Arrhenius plot for pure Ag powder showed a convex-upward curve above 473 K. This is due to a large oxygen consumption rate, that is, a large interphase concentration gradient of O_2. Frequent appearance of mass transfer effects as shown in Fig. 7 suggests that the surface reaction rates over Ag · NaCl and Ag/NaCl catalysts would be fairly close to the rates of interphase diffusion processes.

Experimental results providing some mechanistic information are given in Fig. 8. The discrepancy in carbon balance was ~2% in each pulses. In the first pulse, the 2.67×10^{-7} mol of O_2 in the reaction mixture was completely consumed and 95% of it remained irreversibly on the catalyst. Gaseous products were EO, CH_3CHO, and trace amounts of CO_2. As the surface layers had been saturated with adsorbed oxygen, the formation of CO_2 was promoted and that of CH_3CHO decreased, while EO formation was steady after the second pulse. When ORF-1 and ORF-2 were used, CH_3CHO was not produced (*2*). In the absence of gaseous O_2, EO was converted to

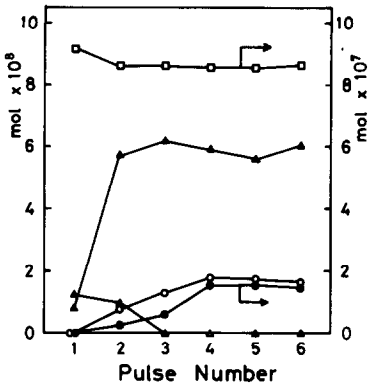

FIG. 8. Variation of product distribution with pulse number when a small pulse size of ERF (50 μl) was used. Catalyst, Cat-Q (0.1 g); reaction temperature, 543 K; He carrier rate, 15 ml min^{-1}. (▲) C_2H_4O, (△) CH_3CHO, (○) CO_2, (□) unreacted C_2H_4, (●) effused O_2.

CH_3CHO and small amounts of C_2H_4 and CO_2. Consequently, the formation of CH_3CHO appears likely to have arisen from the isomerization of EO. If this is correct, the net selectivities to EO are 97 and 91% in the first and second pulses, respectively. But the possibility that CH_3CHO-like species are produced by C_2H_4 adsorption on oxygen adatom is not necessarily rejected. The oxygen adsorbed irreversibly in the earlier pulses would become incorporated into the surface layers by strong ionic interactions with Ag, Na, and Cl. This speculation is firmly supported by the fact that the predominant species in XPS and UPS spectra after the oxygen adsorption of $\sim 3 \times 10^{-9}$ L at 473 K was subsurface oxygen atom (XPS 531.3 eV, UPS 3.5 eV) (*20*). Recently, Grant and Lambert suggested that the presence of subsurface and/or dissolved oxygen atoms promoted EO formation (*21, 22*). It would be valid to consider that the oxygen species is inactive, reduces the mobility of free electrons of metallic Ag, and then forces the top Ag surface to an electron-deficient state, i.e., $Ag^{\delta+}$. Because the direct interaction of $Ag^{\delta+}$ and gaseous O_2 would be expected to be weak, the oxygen adsorbed on the sites seems to be a nondissociative species which possesses mild reactivity. On Ag · NaCl catalysts just after the oxygen adsorption at 473 K, XPS (O 1*s*, 533 eV) and UPS (5.8, 9.8, 12.0 eV) spectra assigned to the oxygen admolecule have been observed in addition to those to the subsurface oxygen and oxygen adatom (*20, 23*). As mentioned earlier, the Ag · NaCl catalysts with large amounts of subsurface oxygen have yielded higher selectivity, which coincides with the maximum expected by the mechanism proposed by Kilty and Sachtler (*3*). On the contrary, for pure Ag powder with low selectivity XPS (O 1*s* 531.0 eV) and UPS (3.5 eV) spectra assigned to subsurface oxygen have been very small compared to those for Ag · NaCl catalysts (*24*).

To attain high selectivity in the commercial processes, trace amounts of organic chlorides have been added to reaction mixtures. The organic chlorides are decomposed on the Ag surface. The chloride ion or chlorine produced would selectively poison strong active sites (*3*) and/or reduce the negative charge of oxygen adsorbed on the adjacent sites. Since the commercial Ag catalysts have included alkali metals, the chloride ion can also interact with these metals (perhaps in a metal oxide form) near the top surface. A certain matrix comprising Ag, Na, Cl, and O would then be formed in the surface layers. This situation is considered to be quite similar to the surface structure of the Ag · NaCl catalysts. The catalysts prepared in the present work include amounts of chloride ion larger than those expected to be deposited on the catalyst surface in commercial processes; the same is true for sodium. So, the Ag · NaCl and Ag/NaCl catalysts seem to show lower activity or smaller reaction rates than the commercial catalysts.

ACKNOWLEDGMENTS

The authors are indebted to Professor I. Toyoshima of Hokkaido University, and Professor H. Kanoh and Professor N. Takeno of the Muroran Institute of Technology for their valuable suggestions and experimental support.

REFERENCES

1. Ayame, A., Takeno, N., and Kanoh, H., *J. Chem. Soc. Chem. Commun.* **1982,** 617.
2. Ayame, A., Kimura, T., Yamaguchi, M., Miura, H., Takeno, N., Kanoh, H., and Toyoshima, I., *J. Catal.* **79,** 233 (1983).
3. Kilty, P. A., Rol, N. C., and Sachtler, W. M. H., *in* "Proceedings, 5th International Congress on Catalysis, Palm Beach, 1972" (J. W. Hightower, Ed.), Paper 64. North-Holland, Amsterdam, 1973; Kilty, P. A., and Sachtler, W. M. H., *Catal. Rev.-Sci. Eng.* **10,** 1 (1974).
4. Japan Patent, 50-90591.
5. Twigg, G. H., *Proc. R. Soc. London Ser. A* **188,** 92,105,123 (1946).
6. Margolis, L. Ya., "Advances in Catalysis," Vol. 14, p. 429. Academic Press, New York, 1963.
7. Ayame, A., Kanoh, H., and Kanazuka, T., *Mem. Muroran Inst. Technol.* **7,** 55 (1970).
8. Ayame, A., and Kanoh, H., *Nippon Kagaku Kaishi,* **1972,** 1819.
9. Metcalf, P. L., and Harriott, P., *Ind. Eng. Chem., Process. Des. Dev.* **11,** 478 (1972).
10. Ayame, A., Shibuya, Y., Yoshida, T., and Kanoh, H., *Nippon Kagaku Kaishi,* **1973,** 2063.
11. Ayame, A., Numabe, A., Watanabe, Y., and Kanoh, H., *Nippon Kagaku Kaishi,* **1973,** 2071.
12. Ayame, A., Suzuki, Y., and Kanoh, H., *Nippon Kagaku Kaishi,* **1973,** 1792.
13. Japan Patent, 49-30286 and 50-74589 (Shell Int. Res.).
14. Feller-Kniepmeier, M., Feller, H. G., and Titzenthaler, E., *Ber. Bunsenges. Phys. Chem.* **71,** 606 (1967).
15. Seiyama, T., Kagawa, Sh., and Kurama, K., *Kogyo Kagaku Zasshi* **70,** 1137 (1967).
16. Presland, A. E. B., Price, G. L., and Trimm, D. L., *J. Catal.* **26,** 313 (1972).
17. Ayame, A., Miura, H., Kimura, T., Yamaguchi, M., Kanoh, H., Miyahara, K., and Toyoshima, I., *J. Res. Inst. Catal., Hokkaido Univ.* **32,** 49 (1984).
18. Wu, J. C., and Harriott, P., *J. Catal.* **39,** 395 (1975).
19. Kanoh, H., Nishimura, T., and Ayame, A., *J. Catal.* **57,** 372 (1979).
20. Miura, H., Ayame, A., Kanoh, H., Miyahara, K., and Toyoshima, I., *Shinku* **26,** 406 (1983).
21. Grant, R. B., and Lambert, R. M., *J. Catal.* **92,** 364 (1985).
22. Grant, R. B., and Lambert, R. M., *J. Catal.* **93,** 92 (1985).
23. Ayame, A., et al., *unpublished.*
24. Miura, H., Ayame, A., Kanoh, H., Miyahara, K., and Toyoshima, I., *Shinku* **25,** 302 (1982).